Lasers in Eng., Vol. 53, pp. 121–136
Reprints available directly from the publisher
Photocopying permitted by license only

Development of a Rotating Portable Single-layer Laser Scanner

L-Z-H. ZHONG[1,†], T-X. CAO[1,†], J-Y. LI[1], Z-J. YI[1], S-F WANG[1,2] AND R ZHENG[1,*]

[1]*School of Optoelectronic Engineering, Changchun University of Science and Technology, 7089 Weixing Rd, Chaoyang District, Changchun 130022, Jilin Province, China*
[2]*Zhongshan Institute of Changchun University of Science and Technology, 16 Huizhan East Rd, Torch Development District, Zhongshan 528437, Guangdong Province, China*

At present, spatial reconstruction is more and more widely used in areas such as environmental perception. Because multi-layer laser scanners have a certain elevation angle, there are blind areas that cannot be scanned during the reconstruction process. This paper proposes a full-circle spatial reconstruction system using single-layer laser scanner to solve this problem, and introduces its hardware structure, spatial coordinate algorithm and statistical outlier removal algorithm. To this end, a series of experiments are built to compare with a 16-layer laser scanner, combining the rotating drive structure to reconstruct the space of the room and single objects. The experiments show that the system not only has better completeness of spatial reconstruction effect than 16-layer laser scanner, at the same time, there is no missing detection space, and the cost is much lower than 16-layer laser scanner. The data processing steps such as feature point extraction and outlier removal of the system are all processed by the Nvidia Jetson AGX Xavier mini-workstation and then the scanning point cloud images are output through the serial port.

Keywords: Single-layer laser scanner, rotating drive structure, spatial reconstruction, spatial coordinate algorithm, statistical outlier removal algorithm

1 INTRODUCTION

Artificial intelligence (AI) within the unmanned vehicle industry has developed rapidly in recent years and, with it, the use of laser scanners for spatial

*Corresponding author: E-mail: zhengru@cust.edu.cn
† L. Z. H. Zhong and T. X. Cao contributed equally to this work.

reconstruction of the surrounding environment has become extremely important. The technology of a laser scanner for spatial reconstruction of the surrounding environment is widely used in the unmanned vehicle industry [3], as well as in dangerous and unknown environments that are not suitable for human exploration. [4].

While single-layer laser scanner can only scan planes, a 16-layer laser scanner can perform spatial scanning, but its existence of a certain elevation angle will cause it to have scanning blind spots [2]. This paper presents the design of a new spatial scanning system based on single-layer laser scanner which can achieve the spatial reconstruction of single-layer laser scanner and has the advantage of low cost. This design is based on a 360° rotating single-layer laser scanner and combines the spatial coordinate algorithm with the statistical outlier removal algorithm to perform spatial reconstruction. The initial spatial reconstruction of single-layer laser scanner used a stepper motor. Its large size and heavy weight can only be used for spatial reconstruction on the z-axis plane and at a fixed location, which cannot meet the needs of current spatial reconstruction [1].

Based on the above analysis of the problems and requirements, we present a set of rotating drive structure is designed to enable the single-layer laser scanner to achieve 360° rotation in the z-axis and y-axis planes for spatial reconstruction. The design is small, portable, can be handheld for spatial reconstruction and does not need to be combined with an internal measurement unit (IMU). The system is built for experimental data acquisition and processing, and the spatial reconstruction of the environment by single-layer laser scanner is completed.

2 SPATIAL RECONSTRUCTION LASER SCANNER COMPOSITION

2.1 Round rod connecting rod structure

The round rod connecting rod structure is used to fix the whole hardware centre and connect the various parts of the mechanical parts (see Figure 1). The round rod connecting rod structure is more convenient to connect and it is more conducive to disassembling the entire structure of the portable laser scanner. In addition, the round rod connecting rod structure plays the role of lubrication to ensure that the device will not be stuck when it is working.

2.2 Bearing sleeve

Bearing sleeves are widely used in light load and easy to disassemble scenarios. Applying the bearing sleeve to our equipment will help us to more easily disassemble and assemble when working outdoors, reduce the carrying volume and facilitate outdoor work (see Figure 2 and Figure 3). Many bearings will encounter difficulties in assembly and disassembly, especially when the assembly of the bearing inside the box is restricted by conditions. The

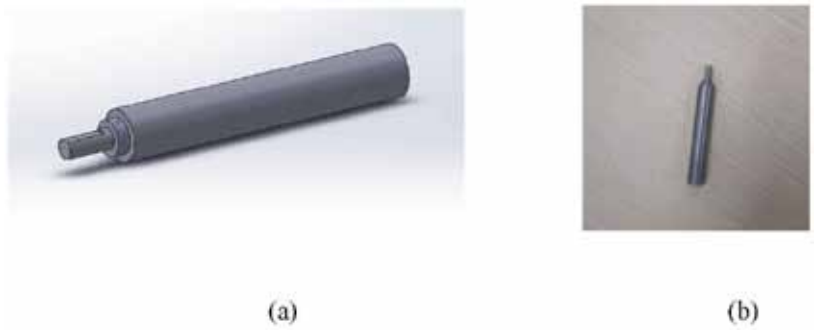

FIGURE 1
(a) Technical rendering of the round bar connecting rod and (b) photograph of the actual round bar connecting rod.

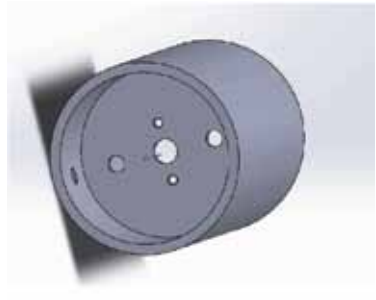

FIGURE 2
Model of the bearing sleeve.

FIGURE 3
Photograph of the bearing sleeve.

application of bearing sleeve can solve the problem of assembly and disassembly, and the bearing sleeve can be adjusted tightly and loosely, which greatly reduces the occurrence of component dislocation due to violent movement of the device. The most important role of the bearing sleeve in the machinery is to fix the rod to stabilize the laser scanner. When the gear shaft is moving, use the bearing sleeve to help fix it, and try not to let it appear direction deviation due to vibration. In this way, the whole structure can be made more stable, which is convenient for outdoor hand-held work and other activities.

2.3 Slip ring

The slip ring (MT1233; Moflon Technology Company, Ltd.) is an electrical component responsible for connecting and transmitting energy and signals for the rotating body (see Figure 4). The rotating part is connected to the rotating structure of the equipment and rotates therewith, called the rotor and the stationary part is connected to the energy source of the fixed structure of the equipment, called the stator. The overall structure relies on the principle of elastic lap joint, rolling lap joint principle and sealing principle, as well as ingenious movement structure and sealing structure design, forming a stable and reliable rotating connection system. Install the slip ring on the bearing sleeve and connect the data line and power line of the laser scanner to the wire on the slip ring, so that the laser scanner can rotate infinitely while detecting its rotation state. The wire on the rotating shaft of the slip ring is connected with the data line and power line of the laser scanner, so the wires will not be entangled due to the rotation of the laser scanner during operation.

2.4 Geared motor

The geared motor (RC370-0660-36; Shenzhen Tianqu Electronics Company, Ltd.) is indirectly connected to the laser scanner to make the laser scanner

FIGURE 4
Slip ring model diagram.

rotate 360° in space for mapping work (see Figure 5 and Figure 6). It has high efficiency and reliability, long working life and easy maintenance. It has low energy consumption, low vibration, low noise, superior performance, and the efficiency of the reducer is as high as 96%. At the same time, the motor can also adjust the speed, adjust the speed of the whole device, and the accuracy and speed of mapping. Based on the requirements of various applications, choosing this geared motor can adjust the motor speed, and cooperate with the work of the laser scanner, so that the overall work efficiency and the effect of image modelling are more perfect. A rendered drawing of the round rod connecting rod, bearing sleeve, slip ring and geared motor installation is shown in Figure 7.

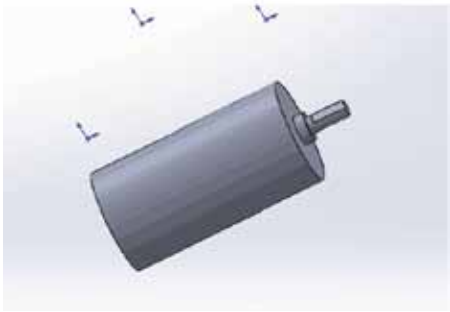

FIGURE 5
Model of the geared motor.

FIGURE 6
Photograph of the geared motor.

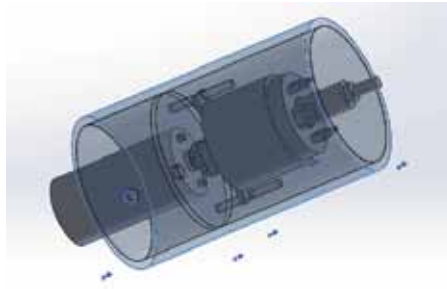

FIGURE 7
Rendered diagram of the rotating drive structure.

2.5 Single-layer laser scanner

A laser scanner analyses the reflected energy on the surface of the target object, the amplitude, frequency and phase of the reflected spectrum by measuring the propagation distance between the sensor transmitter as well as the target object, and then presents accurate spatial structure information of the target object. Herein we employed a single-layer laser scanner (UTM-30LX; Hokuyo Automatic Company, Ltd.) distance measurement product, which has a measurement range of 30 m, an angle of 270°, DC 12 V input, 25 ms scanning time, IP64 protection level, non-contact measurement and other performance, which can work in under 1000001× light intensity. It has the characteristics of high precision, high resolution, wide field of view, low weight, and low power consumption. The compact design saves installation space. As the core component of the whole device, the laser scanner is used in this paper, and the algorithm is used in conjunction with the mechanical structure of the handheld part to enable it to achieve spatial reconstruction. Some performance parameters of the single-layer laser scanner are given in Table 1.

TABLE 1
Working parameters of the single-layer laser scanner used in this work.

Power Supply	12 V DC ±10%
Light Source	Semiconductor laser, $\lambda = 905$ nm
Measuring Distance	0.1 to 30 m, Max. 60 m, 270°
Precision	0.1 to 10 m; ±30 mm; 10 to 30 m; ±50 mm
Angle Resolution	0.25° (360°/1,440 steps)
Scan Time	25 msec/scan

2.6 Mini-workstation

The performance of mini-workstation (NVIDIA Jetson AGX Xavier; Shenzhen Yahboom Technology Company, Ltd.) is comparable to that of large workstations, but its volume is only 1/10 of that of workstations, making it easy to carry and debug according to different environments. NVIDIA Jetson AGX Xavier is mainly used for deep neural network reasoning for edge computing, and it supports models derived from various deep learning frameworks such as Caffe, Tensorflow, and PyTorch. In order to further improve the computational efficiency, TensorRT can also be used to Streamlayer and optimize the trained model using computational graph optimization, operator fusion, quantization and other methods. NVIDIA Jetson AGX Xavier enables developers to make full use of computing modules such as Tensor core and deep learning accelerator (DLA) unit in graphics processing unity (GPU) through TensorRT; therefore, the design system of this article selects it for data processing.

2.7 Inverter

An inverter (BEU1000L; Guangzhou Poojin Electronic Company, Ltd.) is a converter that converts DC electric energy (battery, storage battery) into fixed frequency, constant voltage or frequency modulated alternating current (generally 220 V, 50 Hz sine wave), and it mainly supplies power to the entire device. The inverter has high conversion efficiency, fast start-up, and good safety performance. The inverter adopts an all-aluminium shell, which has good heat dissipation performance, hard oxidation treatment on the surface, good friction resistance, and resistance to squeezing or impact from a certain external force. It also has strong adaptability and stability with load. The equipment has sufficient power supply and the overall use time is long.

2.8 Single-chip microcomputer

This work used a one timer and two IO ports of the single-chip microcomputer (STM32F103C8T6; Shenzhen Risym Electronics Company, Ltd.),

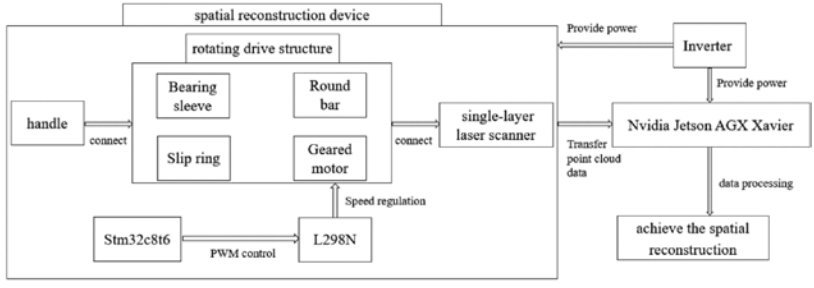

FIGURE 8
Workflow chart of the spatial reconstruction system.

combined with the motor drive module LN298N to adjust the pulse width modulation (PWM) duty cycle, and then change the motor speed to reach a speed of 20 rpm.

2.9 Drive module

A motor drive (L298N; Shenzhen Risym Electronics Company, Ltd.) is mainly used to control motor speed. This work used L298N as the main drive module, which has the characteristics of strong driving ability, low calorific value and strong anti-interference ability. The L298N motor drive module can use the built-in 78M05 chip to obtain power through the drive power supply. In order to avoid damage to the voltage stabilizing chip, when the drive voltage is greater than 12 V, the external 5 V logic power supply is used. When the drive voltage is greater than 12 V, the external 5 V logic power supply is used.

Through the above modules, this article constructs a new full circle spatial reconstruction system, and its workflow is as follows:

3 DESIGN APPROACH AND EXPERIMENTAL METHODOLOGY

3.1 Rotating drive structure

The traditional method is to combine the single-layer laser scanner with an internal measurement unit (IMU) to achieve spatial reconstruction in the environment [5]. The IMU collects the rotation angle of the single-layer laser scanner. The design detailed herein does not need to be combined with IMU but fixes the UTM-30LX single-layer laser scanner onto the rotating shaft of the round rod, the geared motor drives the round rod, and the round rod drives the single-layer laser scanner to rotate clockwise. This work used geared motors, slip rings, bearing sleeves, round bars, single-layer laser scanner and handles combined to form a spatial scanning device. The physical connection diagram is shown in Figure 9.

3.2 Space coordinate algorithm

The spatial coordinate algorithm is combined with the characteristics of the UTM-30LX single-layer laser scanner to calculate the spatial coordinates of the point cloud rotated to other angles of the laser scanner according to the data points of each frame, scanning cycle, rotation time of one cycle, and the measured distance data [8].

Suppose there are $n'(n'=1081)$ points in each frame of the UTM-30LX single-layer laser scanner. The time for one scan is, t_1, where t_1=25 ms, the measured distance data is s and the time for the single-layer laser scanner to rotate once is t_2, where t_2=3000 ms. The angle between the two adjacent points of the laser scanner emission and the layer of the laser scanner is given by

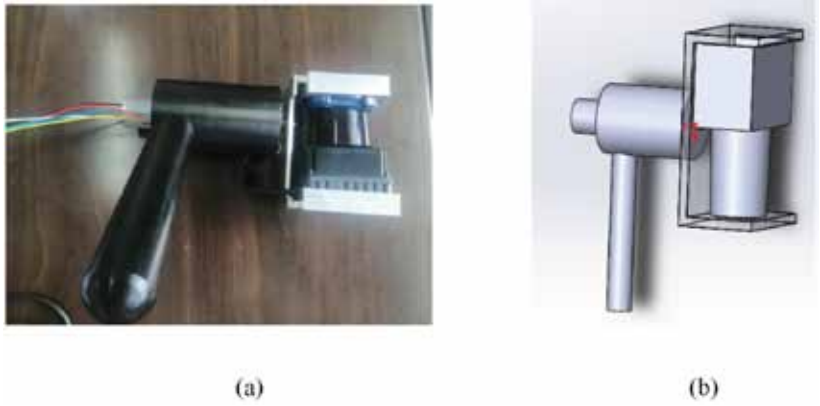

FIGURE 9
(a) Photograph of the spatial scanning device and (b) the simulation diagram.

$$\theta = \frac{270^{\circ}}{n'} \tag{1}$$

The time interval of each point emitted by the laser scanner is

$$h = \frac{t_1}{n'}\# \tag{2}$$

The single-layer laser scanner rotates by angle, h, in time, c:

$$k = 360^{\circ}\frac{c}{t_2}\# \tag{3}$$

If the laser scanner is used as the origin and the front of the laser scanner is used as the x-axis, the right side is used as the y-axis and the upper side is used as the z-axis to establish a rectangular coordinate system. It is easy to know that the angle between the layer of the first point of the laser scanner and the origin of the coordinate and the negative semi-axis of the x-axis is 45°. In this way, the coordinates of the first point of the laser scanner can be written as

$$x = 0 \tag{4a}$$

$$y = -s \times \cos\left(\frac{\pi}{4}\right)\# \tag{4b}$$

$$z = s \times \sin\left(\frac{\pi}{4}\right) \tag{4c}$$

According to the rotation angle, k, the angle θ between the line of the laser scanner and two adjacent points emitted by the laser scanner, the time interval h of each point, the space coordinates of the point cloud at other angles can be calculated in turn.

If the laser scanner rotation axis changes, the coordinates of the changed rotation axis can be calculated according to the angle of the changed rotation axis relative to the current rotation axis, and then the coordinates of each point corresponding to the laser scanner can be calculated.

3.3 Statistical outlier removal algorithm

When laser scanner collects data it will produce measurement errors and individual outliers, which will seriously affect the effect of spatial reconstruction. The statistical outlier removal algorithm can solve this problem [7]. The algorithm filters outliers by statistically judging the distance between the query point and the neighbouring point set and deletes the points that do not meet specific criteria. For each point this paper calculates the average distance from it to all its neighbouring points. The average distance is d_i(i=1, 2, 3, …N) and N is the number of surrounding points. Calculate the average distance as $\overline{x}$ from

$$\overline{x} = \frac{\sum_{i=1}^{N} d_i}{N} \# \tag{5}$$

Determine the best threshold, σ according to the actual situation. Compare σ with the calculated average distance from all its neighbours. The result obtained is a Gaussian distribution whose shape is determined by the mean and standard deviation. The points whose average distance is outside the standard range (defined by the global distance mean and variance) and when $\overline{x} < \sigma$ can be defined as outliers and can be removed from the data set.

4 EXPERIMENTAL VERIFICATION

4.1 Experimental procedures and results

The spatial reconstruction system composed of UT-30LX single-layer laser scanner and the rotating drive structure designed by us perform spatial scanning of the room environment and extracts feature points, and then the system is compared with the 16-layer laser scanner.

In order to verify the results, first select a room and place the single-layer laser scanner in the room for spatial reconstruction. The experimental equipment is shown in Figure 10. The rotating portable single-layer laser scanner designed in this paper can achieve 360° rotation in the z-axis and y-axis planes for spatial reconstruction. This paper is performing spatial reconstruction of the entire room, so this paper choose to use the z-axis as the rotation axis of the stepper motor and the *XOY* horizontal plane as the rotation plane. The angular velocity rotates clockwise and the angle between two adjacent lines is 0.2498°. Because in this work we chose to make the laser scanner scan vertically when the stepping motor rotates on the z-axis the data collected by the laser scanner when the motor rotates for one complete cycle is taken as a frame of point cloud data, so that the whole environment can be achieved spatial reconstruction. Collect the data at the position in Figure 10, and use the spatial coordinate algorithm to convert the collected distance data into coordinates under the spatial rectangular coordinate system, then use the statistical outlier removal algorithm to remove individual outlier points. The results of extracting feature points around the room are shown in Figure 11. The result of extracting feature points from objects with good point cloud data in the room is shown in Figure 13.

4.2 Comparison between our designed system and 16-layer laser scanner

4.2.1 Details and backdrop

For comparison we employed a 16-layer laser scanner (VLP-16; Velodyne Lidar Company, Ltd.) to do exactly the same experiment as the UT-30LX single-layer laser scanner and the effect is shown in Figure 14.

FIGURE 10
Photograph of the experimental device used for the spatial reconstruction system.

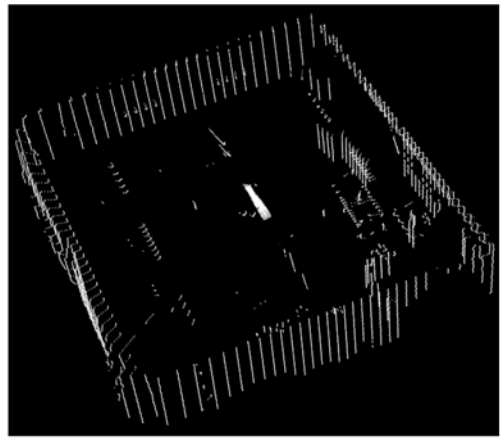

FIGURE 11
Spatial reconstruction of the room.

FIGURE 12
Photograph of the chair in the room.

Comparing the 16-layer effect drawing with the single-layer laser scanner system this paper designed is not difficult to find. Because the elevation angle of the 16-layer laser scanner is ±15° [6], the 16-layer laser scanner will perform spatial reconstruction in a smaller environment. Only part of the environment can be reconstructed. The designed single-layer laser scanner is better than the 16-layer laser scanner in the completeness of the spatial reconstruction.

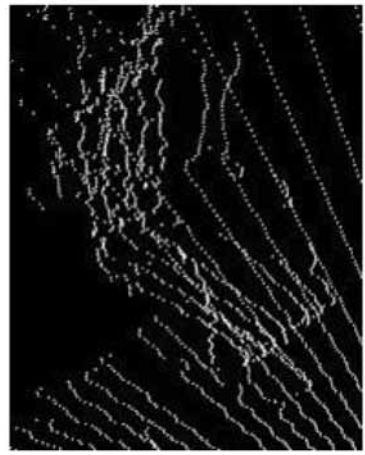

FIGURE 13
Point cloud data diagram of the chair in the room.

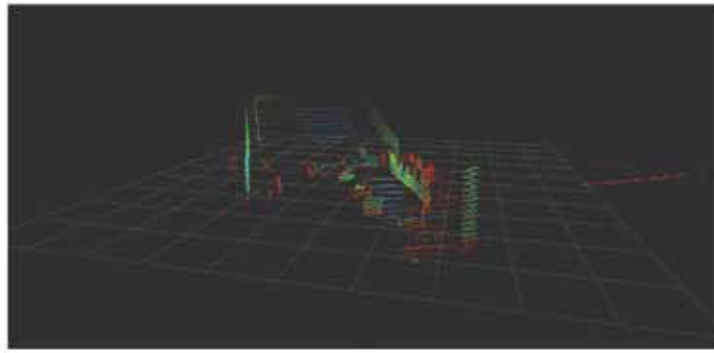

FIGURE 14
Spatial reconstruction achieved with the 16-layer laser scanner.

4.2.2 Blind zone comparison

When the height of the detection space is 3.2 m and the length is 7.25 m, the 16-layer laser scanner is limited by the elevation angle scanning range of ±15°; consequently, the following experiment was conducted to fix the laser scanner height at 1 m and move the distance between the laser scanner and the wall. The 16-layer laser scanner scanning range is 100 m, the room can be covered around. Therefore, the vertical height scanned by the 16-layer laser scanner is compared with the vertical height scanned by the system this paper designed. Suppose the height of the scanned room is y and the distance between the laser scanner placement position and the wall is x, then

$$y = 2x * \tan(15°) \quad 0 < x < 3.732\# \tag{6}$$

and

$$y = 1 + x * \tan(15°) \quad x \geq 3.732 \tag{7}$$

The scanning height data of 16-layer laser scanner can be calculated and the results are shown in Table 2. The system this paper designed can achieve full-circle spatial reconstruction, so the detection range is 360° and the vertical height is 3.2 m. The ratio of the vertical height scanned by the 16-layer laser scanner to the vertical height scanned by the system is used as an index to measure the blind area of the 16-layer laser scanner, and the results are shown in Table 3. It can be seen from Table 3 that the scanning vertical of the 16-layer laser scanner increases with the increase of x. But as x continues to increase there is always a cone-shaped missed space in the space above the 16-layer laser scanner. The design can carry out a full-circle spatial reconstruction of the surrounding environment, and there is no space for missed inspections.

Through the above-mentioned comparison of scanning heights, the scanning effect difference between this system and the 16-layer laser scanner can be reflected from a one-dimensional (1-D) perspective, the blind spot comparison between the two cannot be directly reflected. This work, therefore, places the 16-layer laser scanner in the center position of detection space, the scanning blind area is calculated intuitively, and compared with the detection space volume. The schematic diagram of the 16-layer laser scanner scanning blind area is given in Figure 15. The shaded part in the above figure represents the scanning blind area of the 16-layer laser scanner in the detection space. The volume of the scanning blind area is 112 m^3 and the detection space volume is 194.56 m^3 through calculation. The volume of the scanning

TABLE 2
Scanning height of the 16-layer laser scanner.

Distance, x (m)	1	2	3	4	5	6	7
Height, y (m)	0.5359	1.0718	1.6080	2.0718	2.3397	2.6077	2.8756

TABLE 3
Comparison of detection blind areas.

Height (m)	3.2	3.2	3.2	3.2	3.2	3.2	3.2
Ratio	0.167	0.335	0.503	0.647	0.731	0.815	0.899

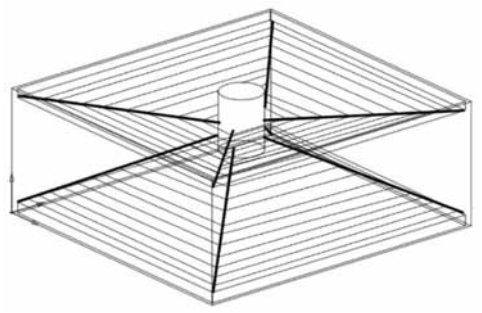

FIGURE 15
Schematic diagram of scanning blind area of the 16-layer laser scanner.

blind area accounts for 57.57% of the detection space volume, and the scanning efficiency is not high; however, this device has a scanning rate of 100% for the detection space, and there is no blind zone for scanning small and medium sized spaces.

4.2.3 Cost comparison

Through the comparison shown in Table 4 it can be seen that the price comparison between this equipment and the multi-layer scanner has obvious advantages.

5 CONCLUSIONS

In the laboratory environment, this paper describes the deployment of a laser scanner on a rotating drive structure composed of geared motors, slip rings, bearing sleeves and other parts. The spatial reconstruction system based on single-layer laser scanner is then placed in different positions of the room to collect data and transmits it to the computer. Then, the two-dimensional (2-D) data is converted into spatial coordinates using the spatial coordinate algorithm and the statistical outlier removal algorithm, thereby achieving the spatial reconstruction. Compared with the 16-layer laser scanner, the angle

TABLE 4
Price comparison data of a single-layer laser scanner and a 16-layer laser scanner.

Single Layer Scanner (UTM-30LX)	Geared Motor and Accessories	16-Layer Laser Scanner
$3,333	$50	$7,000

between the two adjacent layers of the 16-layer laser scanner is 2° and the angle between the two adjacent layers of this design is 0.25°, which contributes to a higher sampling elevation angle and spatial frequency. In the same environment, the scanning blind area is smaller than 16-layer laser scanner, and the cost of this design is much lower than that of 16-layer laser scanner.

In future work the algorithm will be improved and the calculation time will be further optimized to achieve the spatial reconstruction and target recognition of the mobile environment. In addition, a rotating drive system suitable for 16-layer laser scanner is designed to give the 16-layer laser scanner a certain swing to increase its pitch angle and reduce the blind zone range. Also, how to accurately locate and register the 16-layer laser scanner poses a serious challenge. If the existing technology can be further applied to 16-layer laser scanner, the blind area of 16-layer laser scanner scanning will be reduced, so that it can be used in the field of unmanned driving, the environment perception and so on more accurately and perfectly.

ACKNOWLEDGEMENTS

This work was funded by the International Cooperation Foundation of Jilin Province (20210402074GH). It was also supported by the 111 Project of China (D21009, D17017) and the OptoBot Lab.

REFERENCES

[1] Wang Z.W., Liu C.Y., Fu G.H., Hu Q.L., Niu J.Y. and Wang S.F. Full period three-dimensional (3-D) reconstruction method for a low cost single-layer lidar. *Lasers in Engineering* **49**(4-6) (2021), 271-286.

[2] Han Y., Yuan J., Shi J.S., and Yang D.H. Research on real-time small obstacle detection of 16-layer laser scanner point clouds progress in laser and optoelectronics. Progress in Lasers and Optoelectronics **58**(12) (2021), 487-498.

[3] Sun B.Y. SLAM technology for mobile robots. *Electronic Technology & Software Engineering* **2** (2018), 95. (in Chinese)

[4] Su H.Q. Research on robot SLAM Algorithm for Indoor Unknown Environment. MSc dissertation, Hebei University. 2021. (in Chinese)

[5] Cui H.L. Research on Integrated Positioning and Navigation Technology of Smart Car Based on the Fusion of Laser Scanner and IMU. MSc dissertation, Qilu University of Technology. 2021. (in Chinese)

[6] Zhu F. Research on Depth Completion Technology Based on Multi-layer Laser scanner and Monocular Camera. MSc dissertation, Wuhan University. 2020. (in Chinese)

[7] Chen X.R. Research on Three-dimensional Laser Scanning Point Cloud Data Classification Denoising and Hole Repair Algorithm. MSc dissertation, Changan University. 2017. (in Chinese)

[8] Xie X.N. Research on the improvement of the calculation method of the coordinate transformation model. MSc dissertation, East China University of Technology. 2018. (in Chinese)